Supporting Information

Fluorophore-quencher complexes (Cu^{2+}/Al^{3+}) of coumarin Schiff bases as chemosensor for the detection of L-glutamic acid and L-arginine: *In vitro* and *in vivo* studies

M. Ranjani,[1]G.A.Thiruppathi,[2]V. Keerthana,[3]M. Ramya,[4] P. Kalaivani,[5] S.Selvakumar,[3]R. Shankar, [4]K. Srinivasan,[4] P. Sundararaj[2] and R. Prabhakaran[1*]

[1]*Department of Chemistry, Bharathiar University, Coimbatore 641046, India.*
[2]*Department of Zoology, Bharathiar University, Coimbatore 641046, India.*
[3]*Department of Biochemistry, Bharathiar University, Coimbatore 641046, India.*
[4]*Department of Physics, Bharathiar University, Coimbatore 641046, India.*
[5]*Department of Chemistry, Nirmala College for Women, Coimbatore 641018, India.*

[*]*Corresponding authors: E.mail: rpnchemist@gmail.com; rpnchemist@buc.edu.in* (*R. Prabhakaran*)*; Fax: +91-4222422387; Tel: +91-422-2428319*

MATERIALS AND METHODS

The inorganic salts and L-amino acids were of chemically pure in grade and obtained from commercial sourcesand solvents were purified as per reported procedure.[1] RAAGAmelting point apparatus were used to find out the melting points of the compounds. IR spectra were recorded as KBr pellets in the 400-4000 cm^{-1} range with a JASCO FT-IR instrument. The electronic spectra were recorded in the range 200-800nm by using JASCO V-630 UV-Vis spectrometer. The emission spectra were measured using a JASCO FP-6600 instrument at room temperature. The ^{1}H-NMR studies were carried out in DMSO-d^6 by using Bruker 400 MHz instrument with TMS (tetramethylsilane) as standard. The unit cell refinement, crystal data corrections and collections for **RR1** and **RR2** were done at 296 (2) K using SAINT V8.27B and a graphite monochromator with MoKα radiation (λ = 0.71073Å).[2] The structure was solved by SHELXT[45] direct method, which was refined by full-matrix least-squares on $F^2$with anisotropic displacement parameters for the non-H atoms using SHELXL-2016/6.[3]The Structural identification was performed by the programs PLATON,[4] OLEX2,[5] and WinGX.[6,7]

General procedure for preparation of stock solutions

The colorimetric experiments of **RR1** and **RR2** with variouscations were investigated in ethanol:water (1:4 v/v) at 10 μM concentration. The solution of **RR1/ RR2** and various cations (chloride salts) such as Al^{3+}, Ca^{2+}, Co^{2+}, Cr^{3+}, Fe^{2+}, Cu^{2+}, Mn^{2+}, Ni^{2+}, Zn^{2+},Hg^{2+}, $K^+$and Na^+were

prepared separately using ethanol:water (1:4 v/v) at 10 μM concentration. To each 10 μM concentration of **RR1** and **RR2** solution, different cations were added separately and for these solutions, fluorescence and absorption spectra were recorded. For fluorescence study, the excitation wavelength was 310 nm for **RR1** and350 nm for **RR2** with excitation slit of 2.5 nm and emission slit of 5 nm. The fluorescence and absorption titrations were carried out for **RR1** and **RR2** with $Cu^{2+}$and Al^{3+} ions (chloride salts) at 10μM concentration in ethanol:water medium. Job's plot was plotted against **RR1** and **RR2** versus mole fraction of $Cu^{2+}$and Al^{3+} ions respectively.

10 μM solution of **RR1-Cu^{2+}**and **RR2-Al^{3+}**with various L-amino acids such as (Alanine (Ala), Valine (Val), Asparagine (Aspara), Leucine (Leu), Aspartic acid (Asp), Arginine (Arg), Glutamic acid (Glu), Histidine (His), Phenylalanine (Phenylala), Proline (Pro),Methionine (Met) and Threonine (Thr))in ethanol:water (1:4 v/v) were prepared and investigated. To each **RR1-Cu^{2+}**and **RR2-Al^{3+}**solution, various L-amino acids were addedseparately and fluorescence and absorption spectra were recorded. For fluorescence study, the excitation wavelength was 320 nm for **RR1-Cu^{2+}**and390 nm for **RR2-Al^{3+}**with excitation slit of 2.5 nm and emission slit of 5 nm. The fluorescence and absorption titrations were carried out for **RR1-Cu^{2+}** with L-arginine and **RR2-Al^{3+}**withL-glutamic acid at 10μM concentration in ethanol:water (1:4 v/v). Job's plot was plotted against **RR1-Cu^{2+}** versus L-arginine and **RR2-Al^{3+}**versus L-glutamic acid.

Live cell imaging studies

MATERIALS AND METHODS

Maintenance of *C. elegans*

Wild-type *C. elegans* strain was grown and maintained on nematode growth media agar plates seeded with *E. coli* strain OP50 at 20°C according to the standardized protocol (Brenner, 1974).[8] To obtain age-synchronized worm populations, culture plates with eggs and gravid hermaphrodites were washed with M9 buffer (6 g Na_2HPO_4, 3 g KH_2PO_4, 5 g NaCl, 0.25 g $MgSO_4.7H_2O$ and 1 L deionized water) and exposed to alkaline hypochlorite (1 mL of 5M NaOH and 1 mL of household bleach) followed by multiple washed with buffer solution. The gathered eggs were incubated in M9 buffer at 20°C overnight to favor hatching.[9]

Fluorescence microscopy and image processing

Age-synchronized young adult worms (30-35 worms/treatment) were exposed to 1 mL PBS buffer solution containing 10 µM compounds for 5 h. After exposure, the worms were washed off from the plates, anesthetized with sodium azide, and mounted on to 2 % agarose padded microscopic slides. Photomicrographs of immobilized live worms were captured using an upright fluorescence microscope (CX43, Olympus, Japan). The captured images were analyzed for fluorescence signals using ImageJ freeware (NIH, Bethesda, MD) by determining the mean pixel intensity, and the acquired data were subjected to one-way analysis of variance (ANOVA) followed by Bonferroni'sposthoc test (SPSS 17, IBM Corporation, NY). Results are presented as the mean ± standard deviation (SD) of three independent biological trials, each performed in triplicate under similar conditions as described.[10]

Cytotoxicity studies

3-(4,5-Dimethylthiazol-2-yl)-2,5-diphenyltetrazolium bromide (MTT) assay[11]

The cells were cultured ($1x10^4$cells/well) with or without the drug (10 µM to 200 µM) for 24h. Then, plated cells were incubated with 3-(4, 5-dimethylthiazol-2-yl)-2 5-diphenyltetrazolium bromide (MTT, Sigma-Aldrich, 0.5 mg/ml) for 4 h at 37˚C. After incubation, the plates were placed for 25 min at room temperature with shaking to achieve the complete dissolution of formazon and the absorbance was measured at 570nm using a UV spectrophotometric plate reader (Multiskan Go, Thermoscientific).

Confocal Microscopic Imaging

Detection of ROS generation and mitochondrial membrane potential (ΔΨm)

Cultured cells (5×10^5) were seeded on a glass cover slips (0.17mm thickness) in a six-well plate and allowed to attach overnight as previously described.[12] On the next day, medium was replaced with fresh medium containing the IC50 concentration of the compound and incubated for 24 h. At the end of incubation, the cover slips were removed from the culture plate and stained with 10 µm DCFH-DA (Sigma-Aldrich) for 30 min to detect the ROS generation. Further coverslips were co-stained with nuclear stain DAPI (Sigma-Aldrich). To remove extra dye, the stained cover slips were washed with 1× PBS and fixed on a microscopic glass slide with fluro-shield,

(Sigma-Alrich). The fluorescent images were captured using a 40× objective under a laser scanning advanced confocal microscope (DST-PURSE (Phase-II), Bharathiar University).

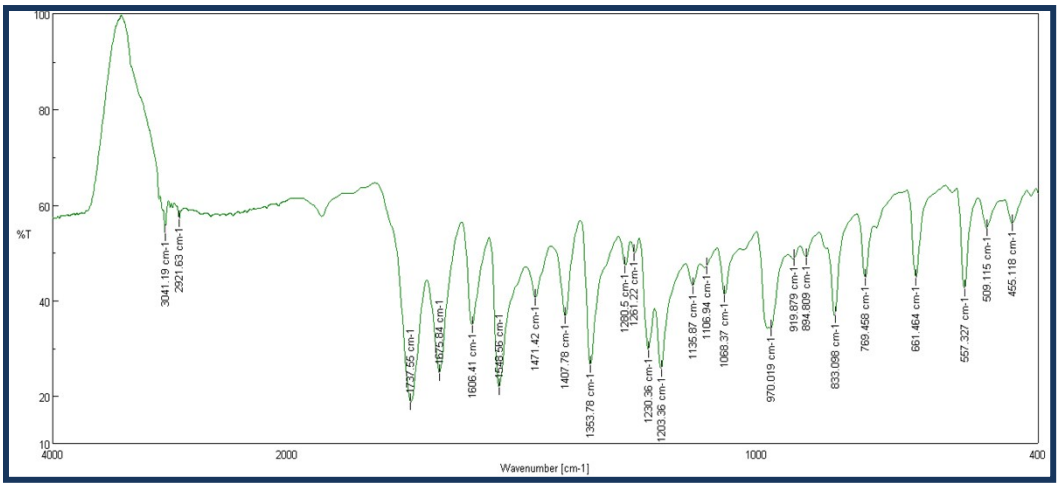

Fig.S1 FT-IR spectrum of Probe (RR1).

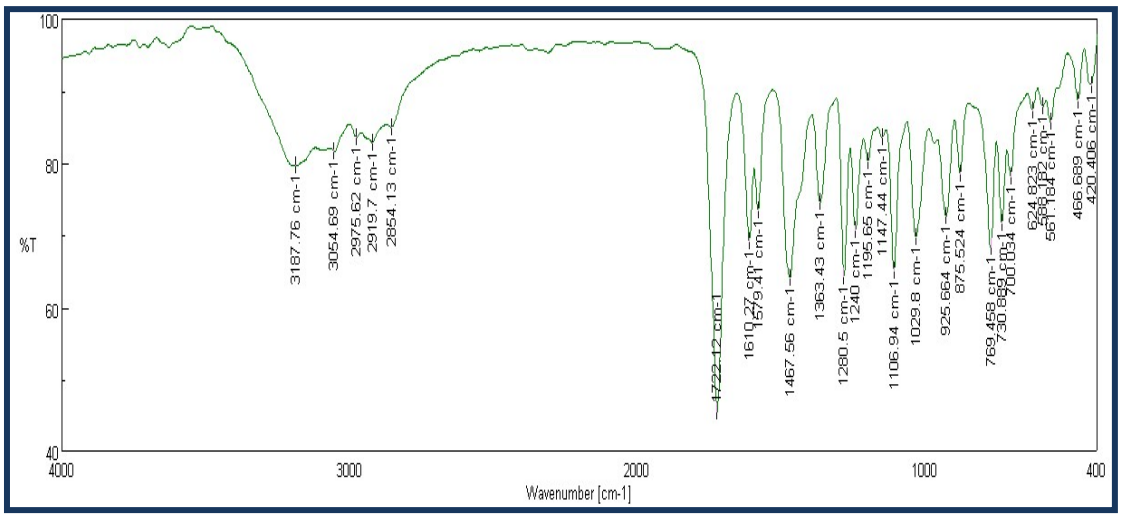

Fig.S2 FT-IR spectrum of Probe (RR2).

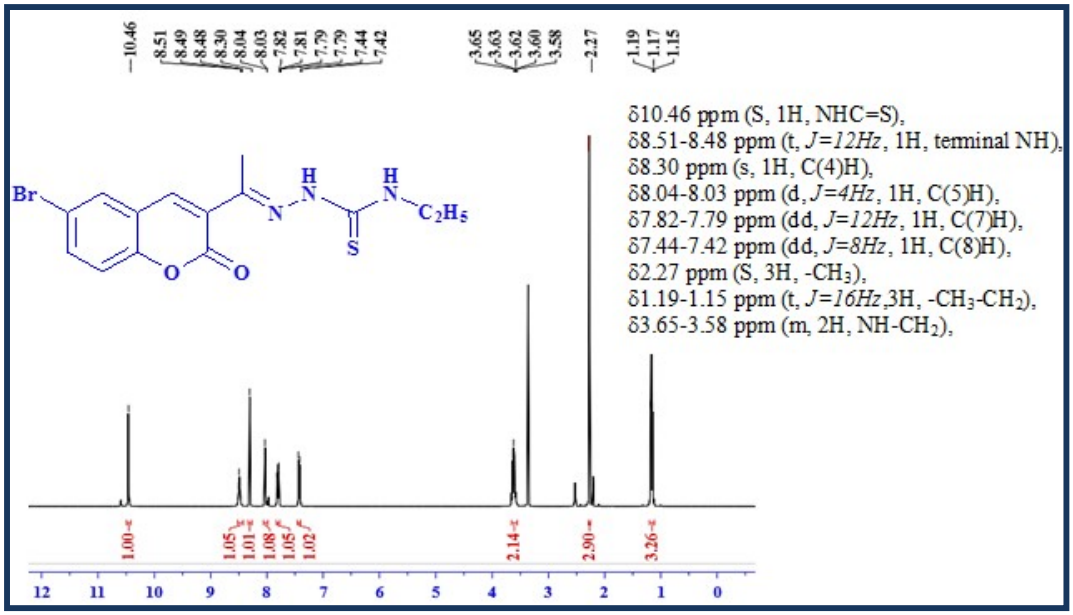

Fig.S3 ^{1}H NMR spectrum of the probe RR1.

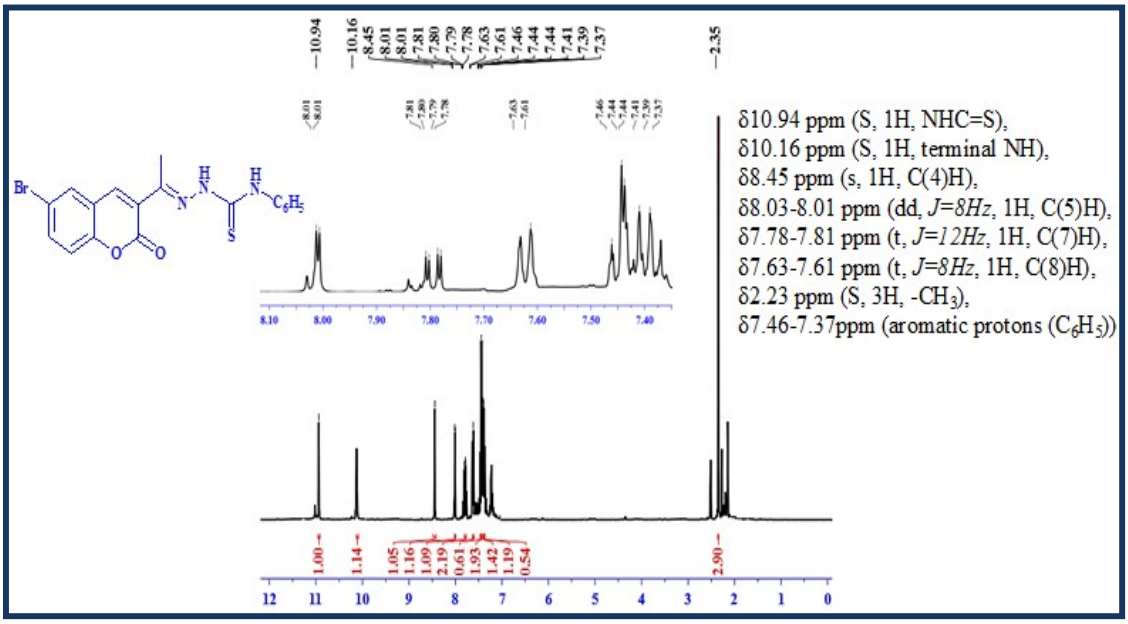

Fig.S4 ^{1}H NMR spectrum of the probe RR2.

Table S1 Crystallographic data of **RR1** and **RR2**

Identification code	**RR1**	**RR2**
Empirical formula	$C_{14}H_{14}BrN_3O_2S$	$C_{18}H_{14}BrN_3O_2S$
Formula weight	368.25	416.29
Temperature	296(2) K	296(2)K
Wavelength	0.71073 Å	0.71073Å
Crystal system	triclinic	monoclinic
Space group	P -1	P 1 21/c 1
Unit cell dimensions		
a	8.059(9)Å	6.886(3) Å
b	10.617(12)Å	12.995(5) Å
c	10.658(12)Å	19.157(7) Å
α	104.79(3)°	90°
β	109.44(3)°	93.108(11)°
γ	106.26(2)°	90°
Volume	761.9(14)Å^3	1711.7(11) Å^3
Z	2	4
Density	1.605 Mg/m^3	1.615 Mg/m^3
Absorption coefficient	2.842mm^{-1}	2.541 mm^{-1}
F(000)	372	840
θ range for data collection	2.19 to 27.11°	2.64 to 27.19°
Limiting indices	-10≤h≤10, -13≤k≤13, -13≤l≤13	-8 ≤ h ≤ 8, -16 ≤ k ≤ 16, -24 ≤ l ≤ 24
Reflections collected	4909	101740
Independent reflections	2596 [R(int) = 0.1049]	3800 [R(int) = 0.0466]
Refinement method	Full-matrix least-squares on F^2	Full-matrix least-squares on F^2
Data/restraints/ parameters	2596 / 0 / 192	3800 / 0 / 236
Goodness-of-fit on F^2	1.003	1.019
Final *R* indices [$I>2\sigma(I)$]	R1 = 0.0816,wR2 = 0.1574	R1 = 0.0329, wR2 = 0.0766
R indices (all data)	R1 = 0.2200, wR2 = 0.2062	R1 = 0.0494, wR2 = 0.0838

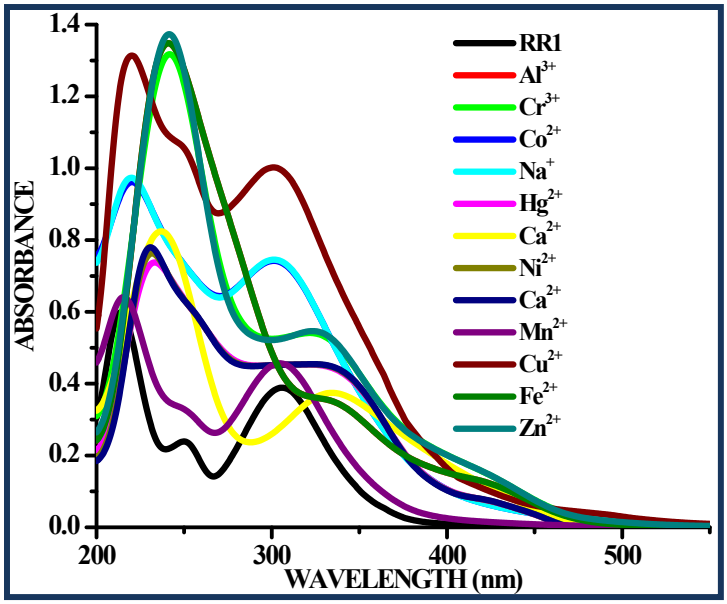

Fig.S5UV-Vis spectra of probe**RR1**in the presence of different cationsat 10 µM concentration in ethanol:water (1:4 v/v).

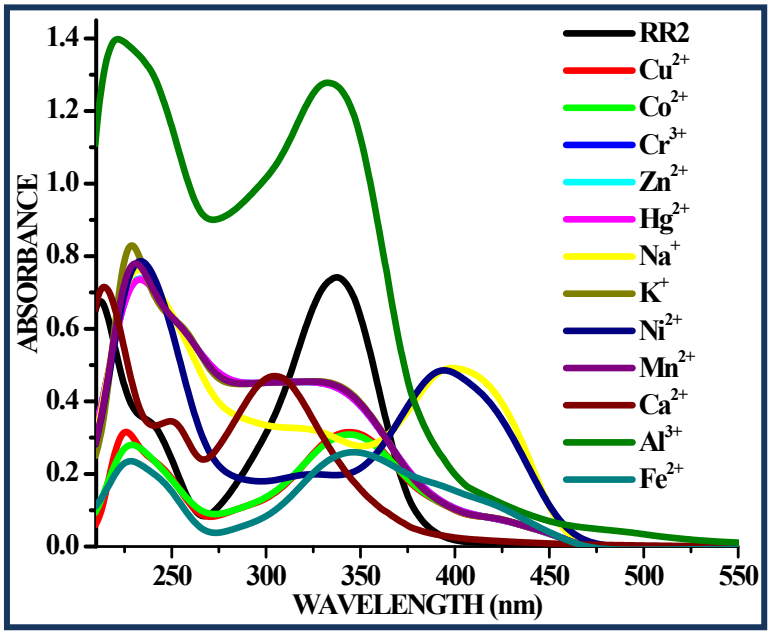

Fig.S6UV-Vis spectra of probe**RR2**in the presence of different cations at 10 µM concentration in ethanol:water (1:4 v/v).

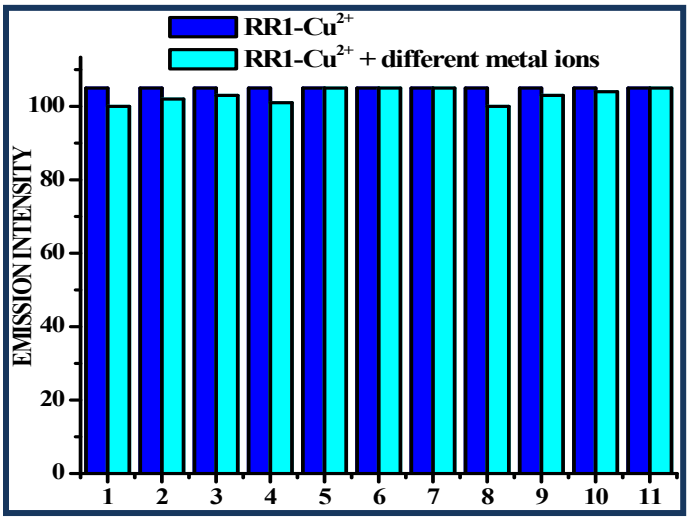

(Fig. S7A) Emission spectra of **RR1-Cu^{2+}**(1 equiv.)with various metal ions (1 equiv.)1- Al^{3+}; 2- Hg^{2+}; 3- Fe^{2+}; 4- Ni^{2+}; 5-Na^{+}; 6- Co^{2+}; 7- Cu^{2+}; 8- Ca^{2+}; 9- K^{+}; 10- $Mn^{2+}$and 11- Cr^{3+}.

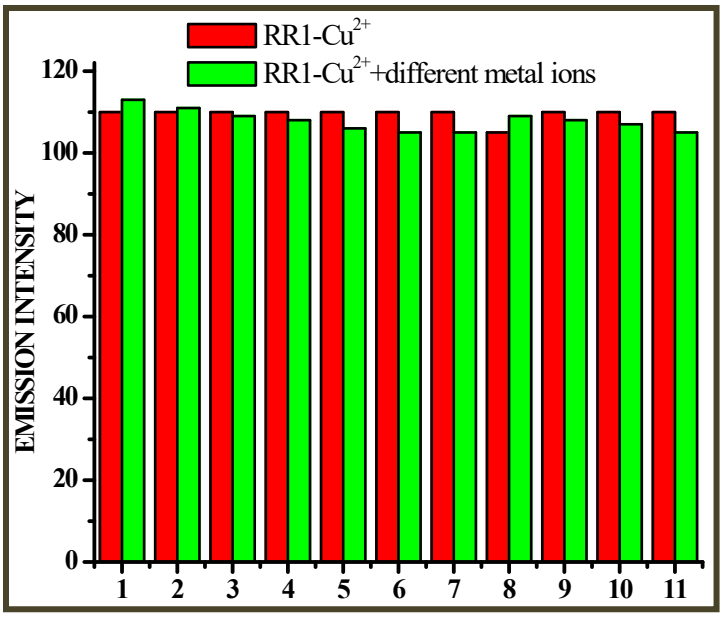

(Fig. S7B) Emission spectra of **RR1-Cu^{2+}**(5 equiv.)with various metal ions (5 equiv.)1- Al^{3+}; 2- Hg^{2+}; 3- Fe^{2+}; 4- Ni^{2+}; 5-Na^{+}; 6- Co^{2+}; 7- Cu^{2+}; 8- Ca^{2+}; 9- K^{+}; 10- $Mn^{2+}$and 11- Cr^{3+}.

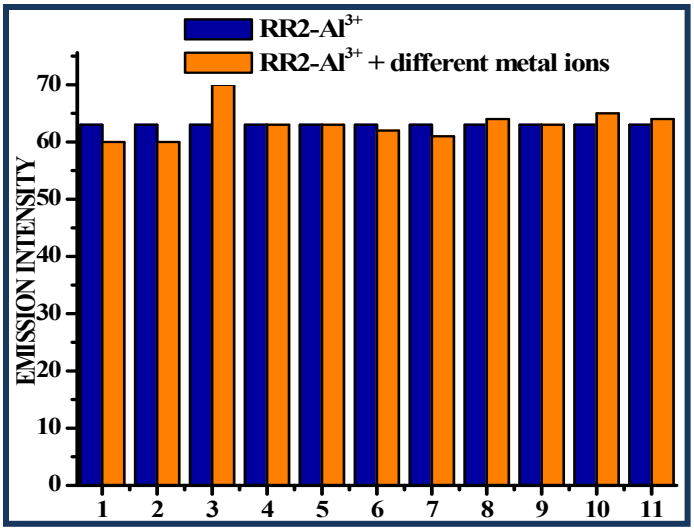

(Fig. S8A) Emission spectra of **RR2-Al^{3+}**(1 equiv.)with various metal ions (1 equiv.)1- Cu^{2+}; 2- Hg^{2+}; 3- Fe^{2+}; 4- Mn^{2+}; 5-K^{+}; 6- Ca^{2+}; 7- Cu^{2+}; 8- Co^{2+}; 9- Cr^{3+}; 10- $Ni^{2+}$and 11- Na^{+}.

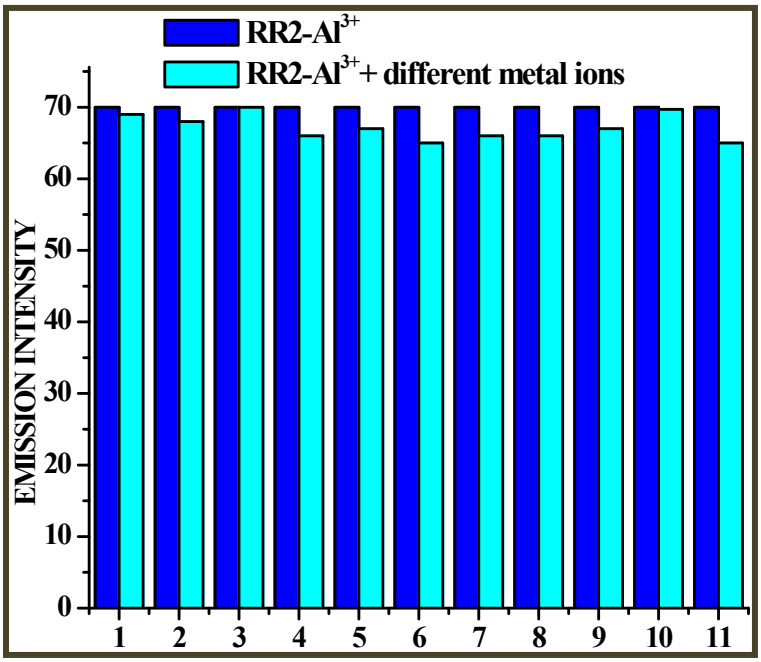

(Fig. S8B) Emission spectra of **RR2-Al^{3+}**(5 equiv.)with various metal ions (5 equiv.)1- Cu^{2+}; 2- Hg^{2+}; 3- Fe^{2+}; 4- Mn^{2+}; 5-K^{+}; 6- Ca^{2+}; 7- Cu^{2+}; 8- Co^{2+}; 9- Cr^{3+}; 10- $Ni^{2+}$and 11- Na^{+}.

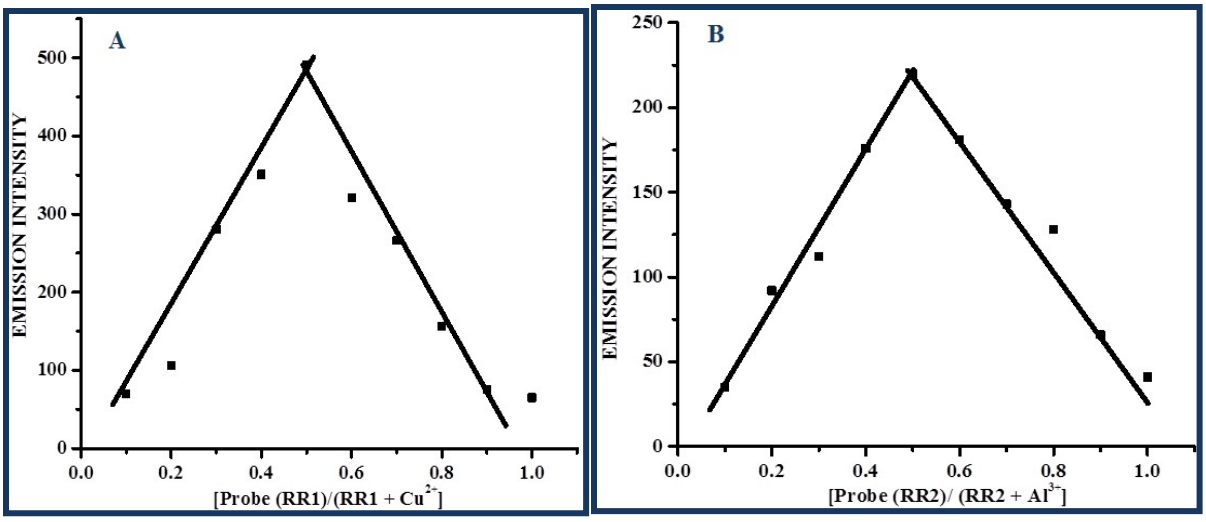

Fig. S9 Job's plot analysis **A**) probe (**RR1**) /[probe (**RR1**)+Cu^{2+} ion] and **B**) probe (**RR2**) / [probe (**RR2**)+Al^{3+} ion]

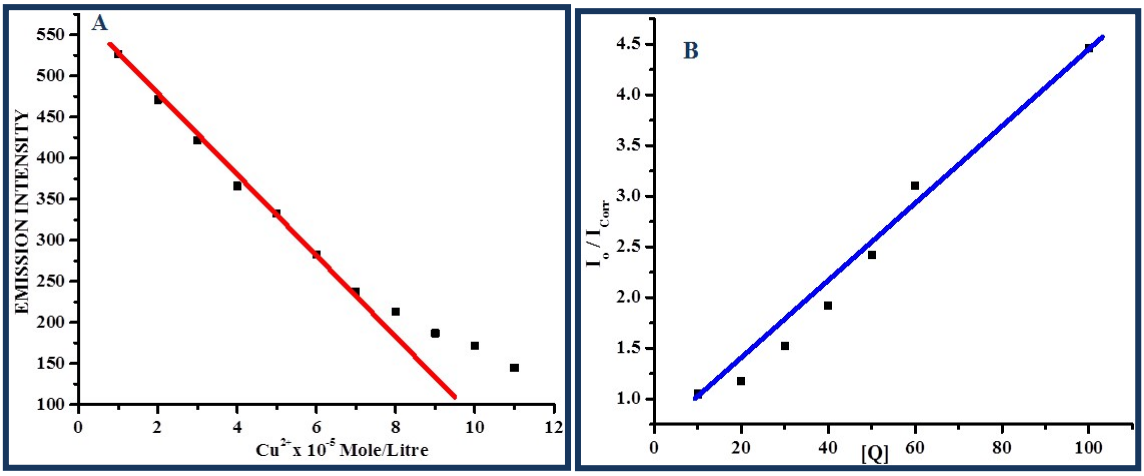

Fig.S10A) Limit of Detection (LOD) plot and **B**) Stern-Volmerplotof**RR1** with Cu^{2+}ions at 10 µM concentration (R^2 = 0.9840).

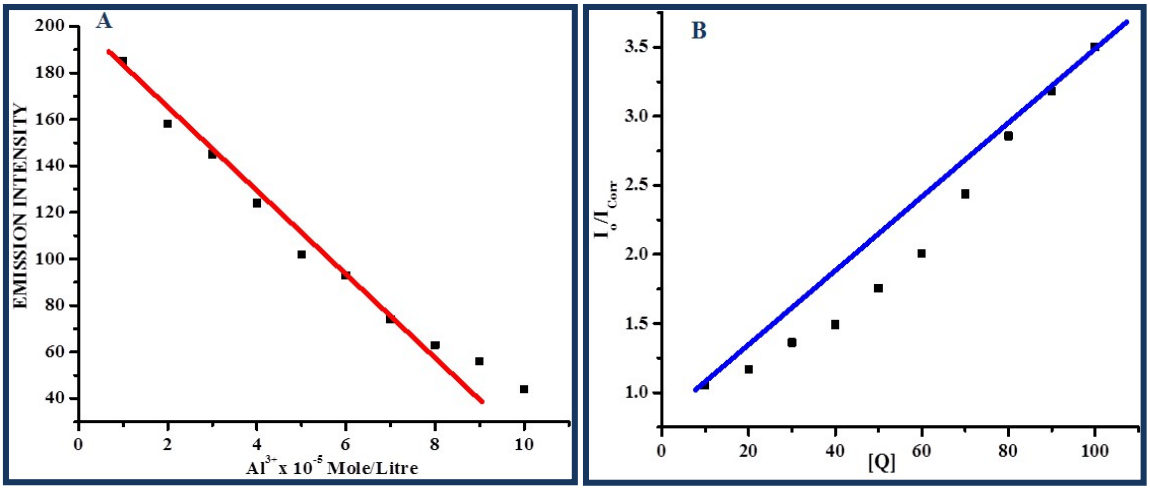

Fig.S11A) Limit of Detection (LOD) plot and **B**) Stern-VolmerplotofRR2 with Al^{3+}ions at 10 µM concentration (R^2 = 0.9671).

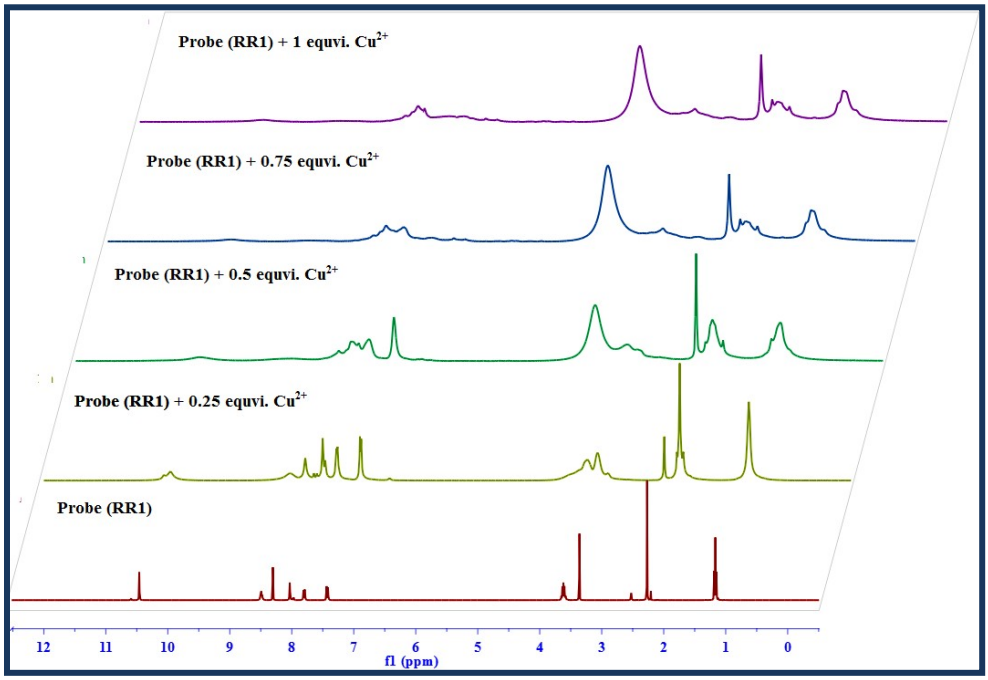

Fig.S12^{1}H-NMR titration spectra of probe **RR1** (1 equiv.) with addition of different concentrations of Cu^{2+} ion using DMSO-d^6 solvent.

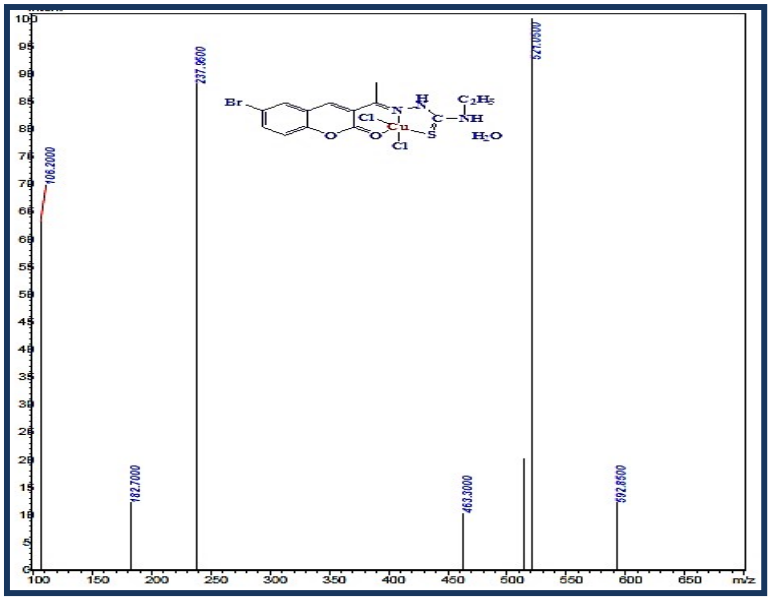

Fig.S13 Mass spectrum of**RR1-Cu^{2+}**.

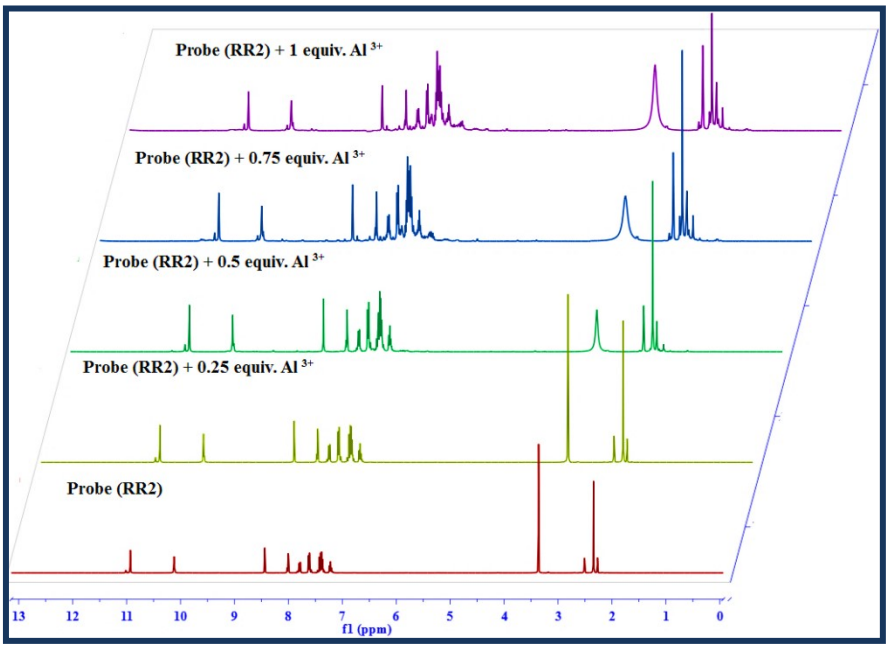

Fig.S14^{1}H-NMR titration spectra of probe **RR2** (1 equiv.) with addition of different concentrations of Al^{3+} ion using DMSO-d^{6} solvent.

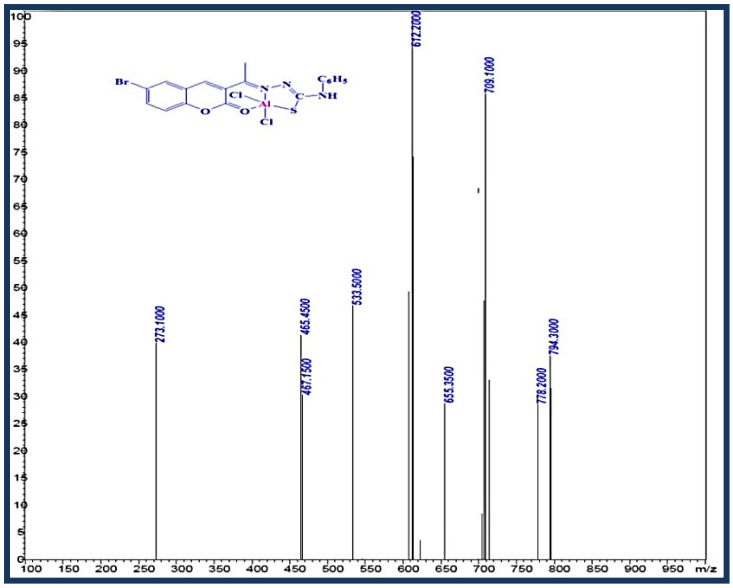

Fig.S15 Mass spectrum of**RR2-Al**$^{3+}$.

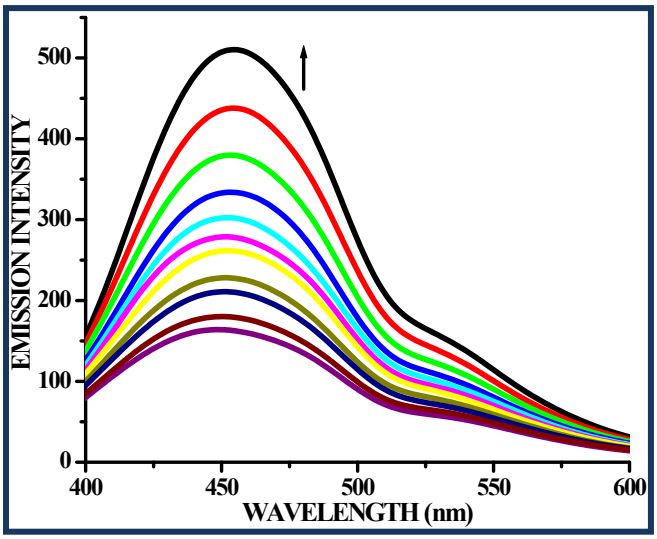

Fig. S16 Changes in emission spectra of **RR1-Cu**$^{2+}$ by increasing the concentration level of L-arginine in ethanol:water (1:4 v/v).

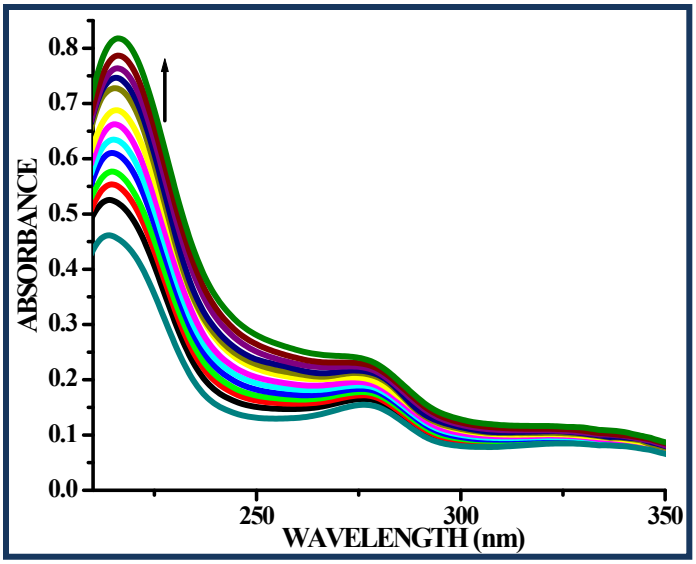

Fig. S17UV-Vis spectra probe **RR1-Cu^{2+}**upon addition of L-arginine at 10 μM concentration in ethanol:water (1:4 v/v).

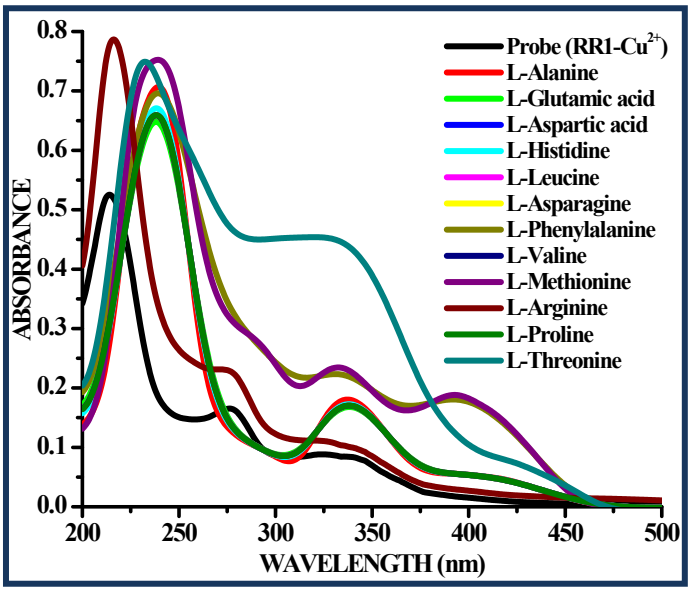

Fig.S18UV-Vis spectra of**RR1-Cu^{2+}**in the presence of different L-amino acids at 10 μM concentration in ethanol:water (1:4 v/v).

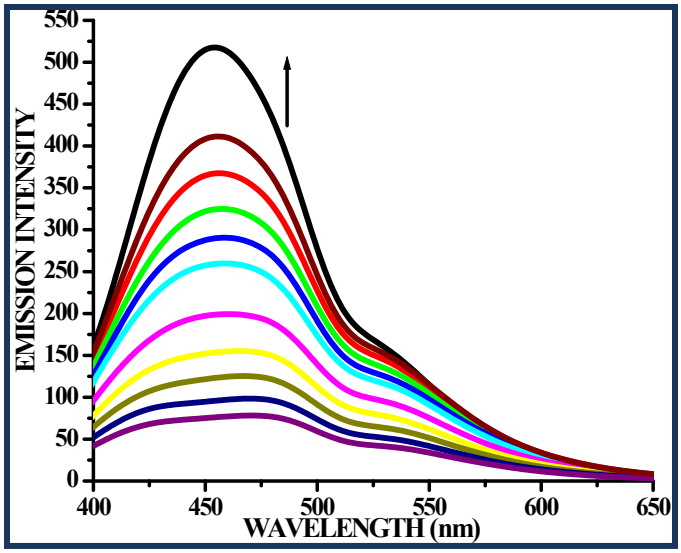

Fig. S19 Changes in emission spectra of **RR2-Al^{3+}**upon addition of L-glutamic acid at 10 μM concentration in ethanol:water (1:4 v/v).

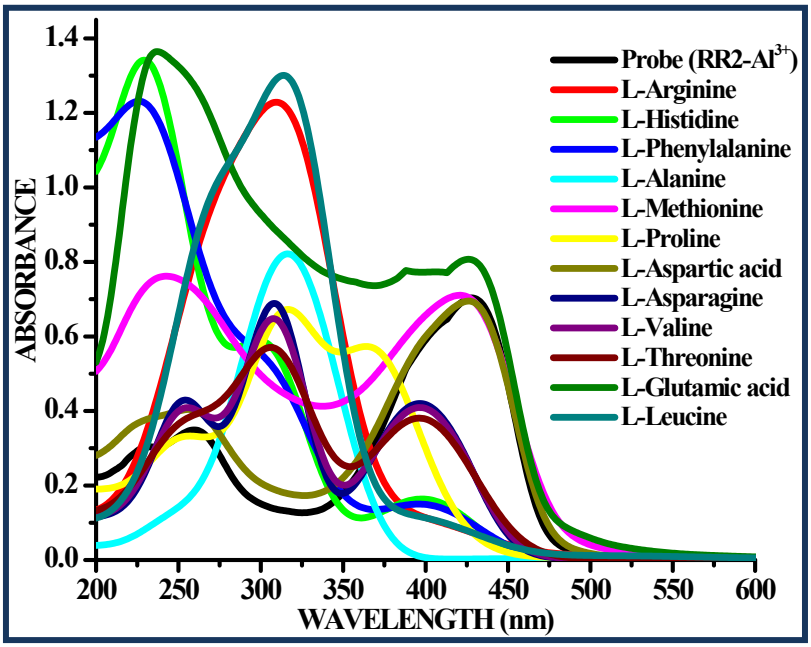

Fig.S20UV-Vis spectra of**RR2-Al^{3+}**in the presence of different L-amino acids at 10 μM concentration in ethanol:water (1:4 v/v).

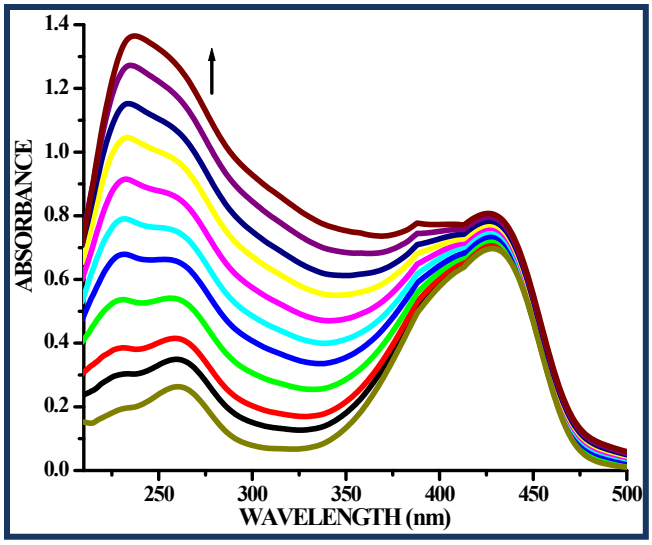

Fig. S21 UV-Vis spectra ofprobe **RR2-Al^{3+}**upon addition of L-glutamic acid at 10 μM concentration in ethanol:water (1:4 v/v).

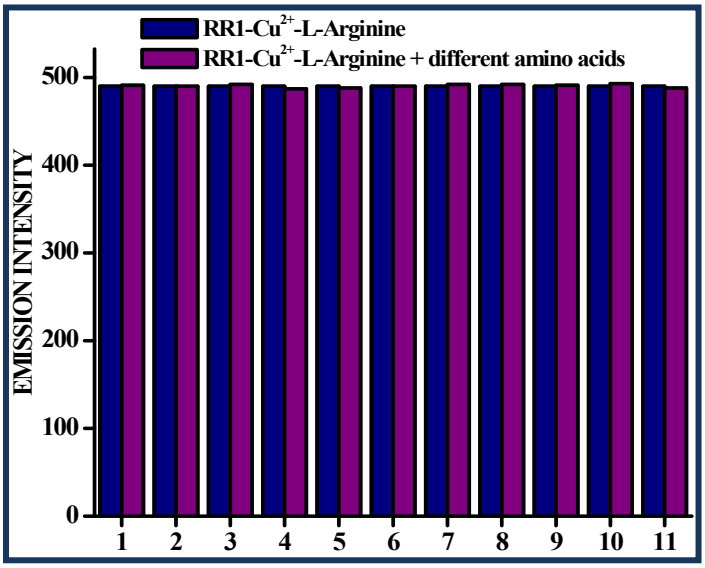

Fig. S22 Emission spectrum of **RR1-Cu^{2+}-L-arginine**(1 equiv.)with various amino acids (1 equiv.)1-L-Aspartic acid; 2-L-Alanine; 3-L-Methionine; 4-L-Glutamic acid; 5-L-Valine; 6-L-Asparagine; 7- L-Leucine; 8-L-Proline; 9-L-Phenylalanine; 10-L-Threonine and 11-L-Histidine.

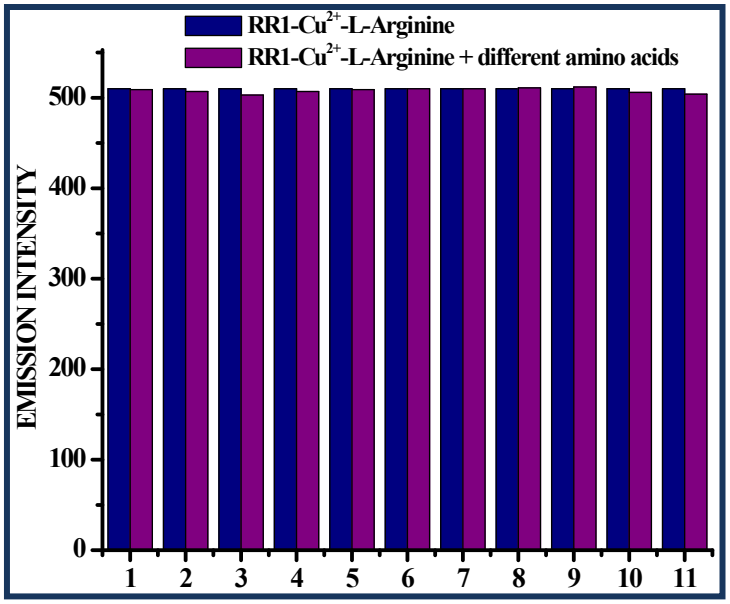

Fig.S23 Emission spectra of**RR1-Cu^{2+}-L-arginine**(5 equiv.)with various amino acids (5 equiv.)1- L-Aspartic acid; 2- L-Alanine; 3- L-Methionine; 4- L-Glutamic acid; 5-L-Valine; 6-L-Asparagine;7- L-Leucine; 8- L-Proline; 9- L-Phenylalanine; 10- L-Threonine and 11- L-Histidine.

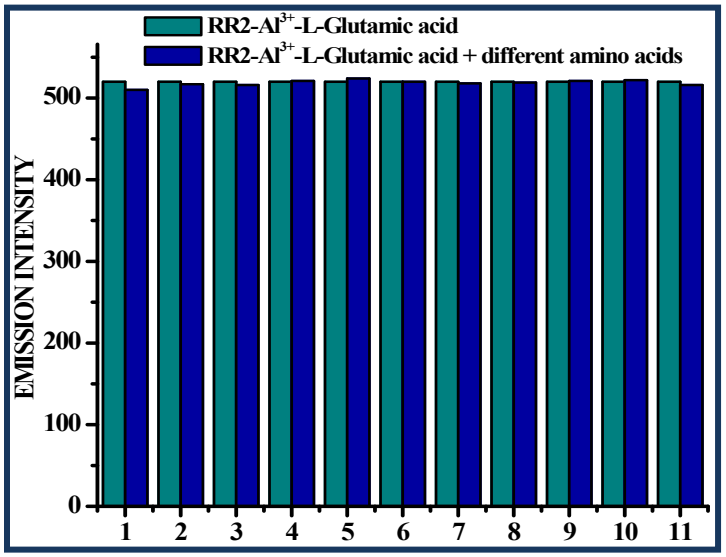

Fig. S24 Emission spectra of **RR2-Al^{3+}-L-glutamic acid**(1 equiv.) with various amino acids (1 equiv.)1-L-Alanine;2-L-Histidine 3-L-Phenylalanine; 4-L-Aspartic acid; 5-L-Valine; 6-L-Threonine;7-L-Methionine; 8-L-Proline; 9-L-Leucine; 10-L-Asparagine and 11-L-Arginine.

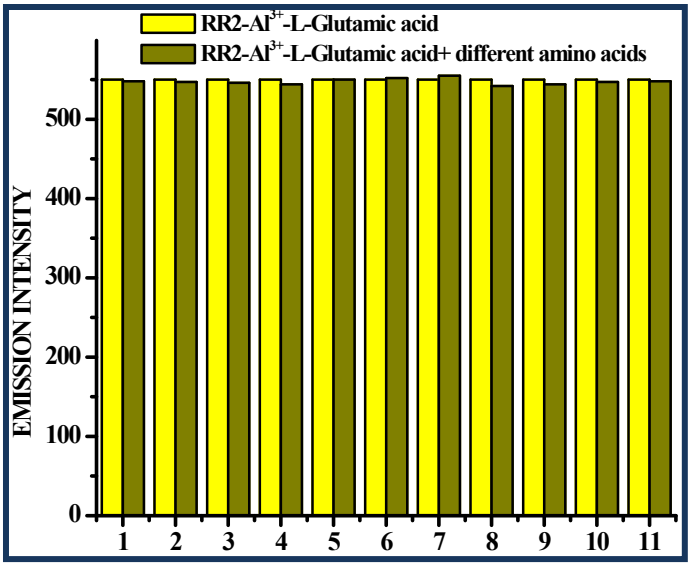

Fig.S25 Emission spectra of**RR2-Al^{3+}-L-glutamic acid**(5 equiv.) with various amino acids (5 equiv.) 1- L-Alanine; 2- L-Histidine 3- L-Phenylalanine; 4- L-Aspartic acid; 5-L-Valine; 6- L-Threonine; 7- L-Methionine; 8- L-Proline; 9-L-Leucine; 10- L-Asparagine and 11- L-Arginine.

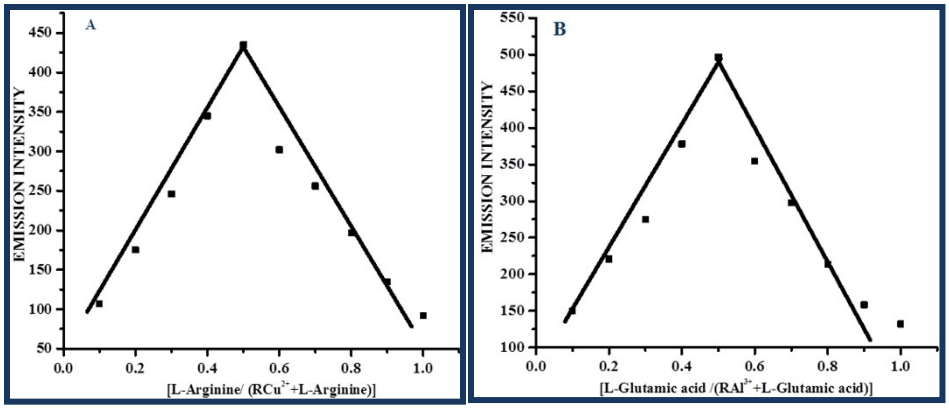

Fig.S26 A) Job's plot of **RR1-Cu^{2+}** and (**RR1-Cu^{2+}-L-arginine**) and **B)** Job's plot of **RR2-Al^{3+}** and (**RR2-Al^{3+}-L-glutamic acid**).

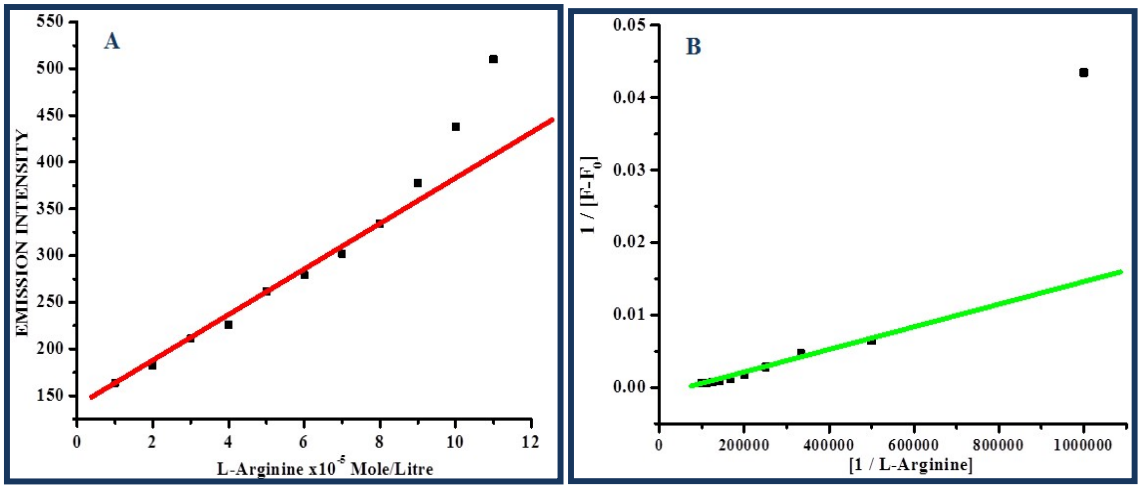

Fig.S27A) Limit of Detection (LOD) plot and **B)**Benesi-Hildebrand (B-H) plot (R^2 = 0.9730) of **RR1-Cu^{2+}** with L-arginine (R^2 = 0.9730).

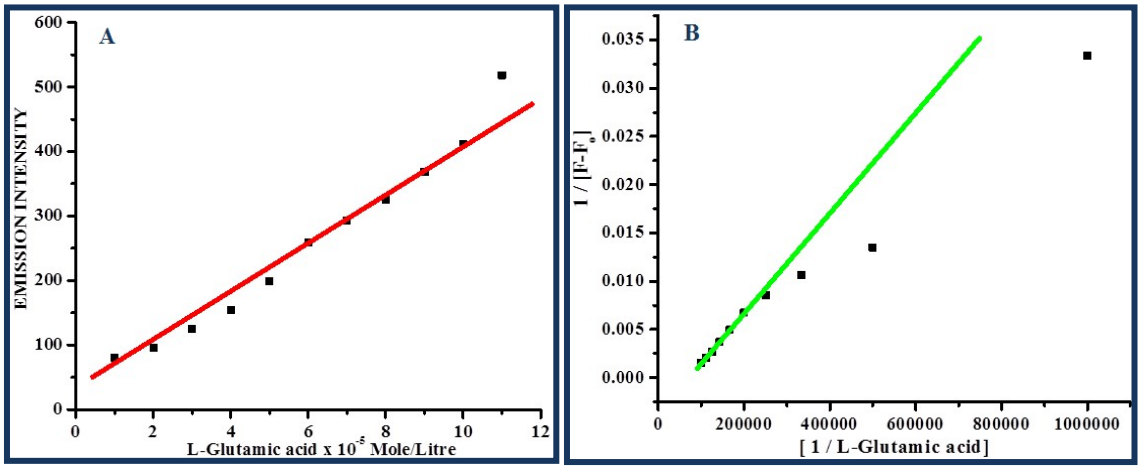

Fig.S28A) Limit of Detection (LOD) plot and **B)**Benesi-Hildebrand (B-H) plot (R^2 = 0.9968) of **RR2-Al^{3+}** with L-glutamic acid.

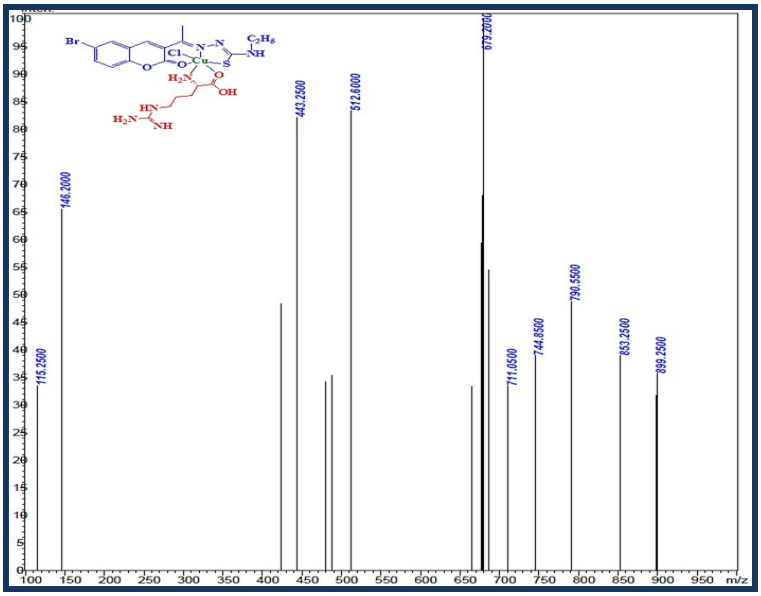

Fig.S29 Mass spectrum of**RR1-Cu^{2+}**-L-arginine.

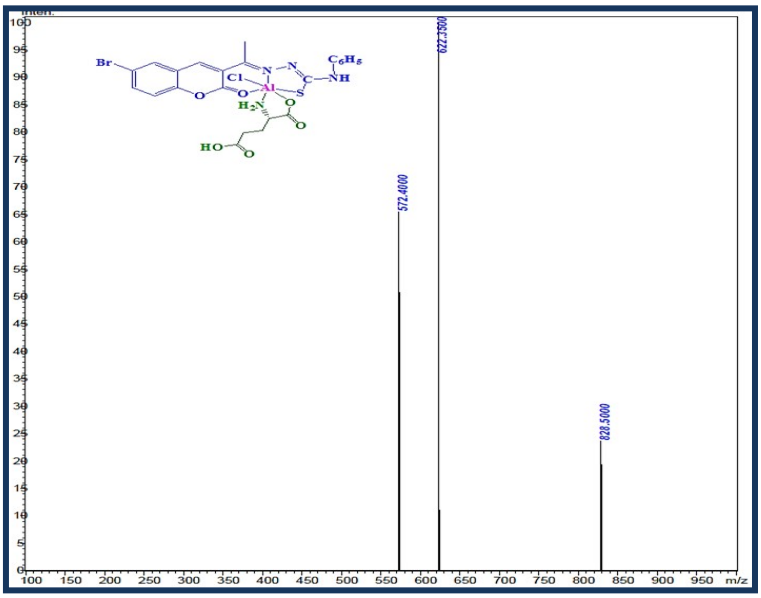

Fig.S30 Mass spectrum of**RR2-Al^{3+}**-L-glutamic acid

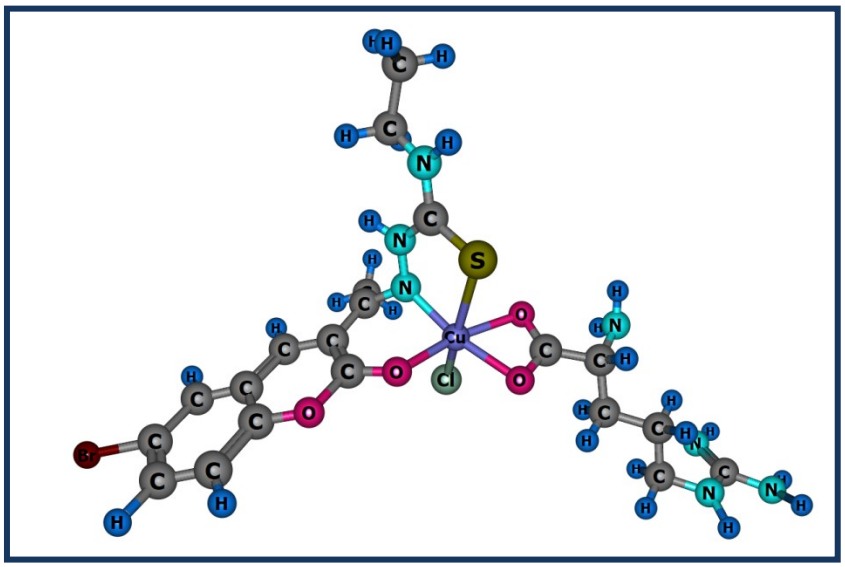

Fig.S31 Optimized structure of the RR2-Cu^{2+}-L-Arginine (B).

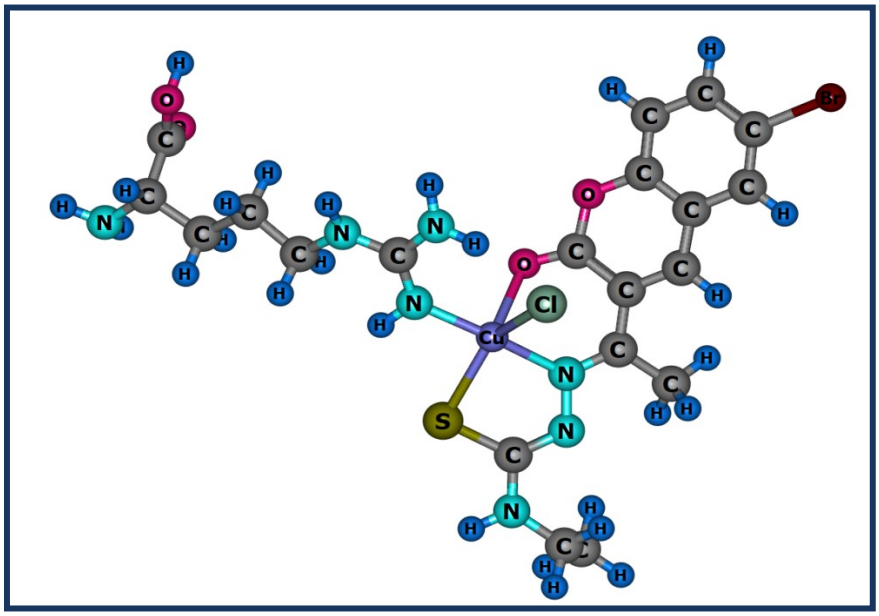

Fig.S32 Optimized structure of the RR2-Cu^{2+}-L-Arginine (C).

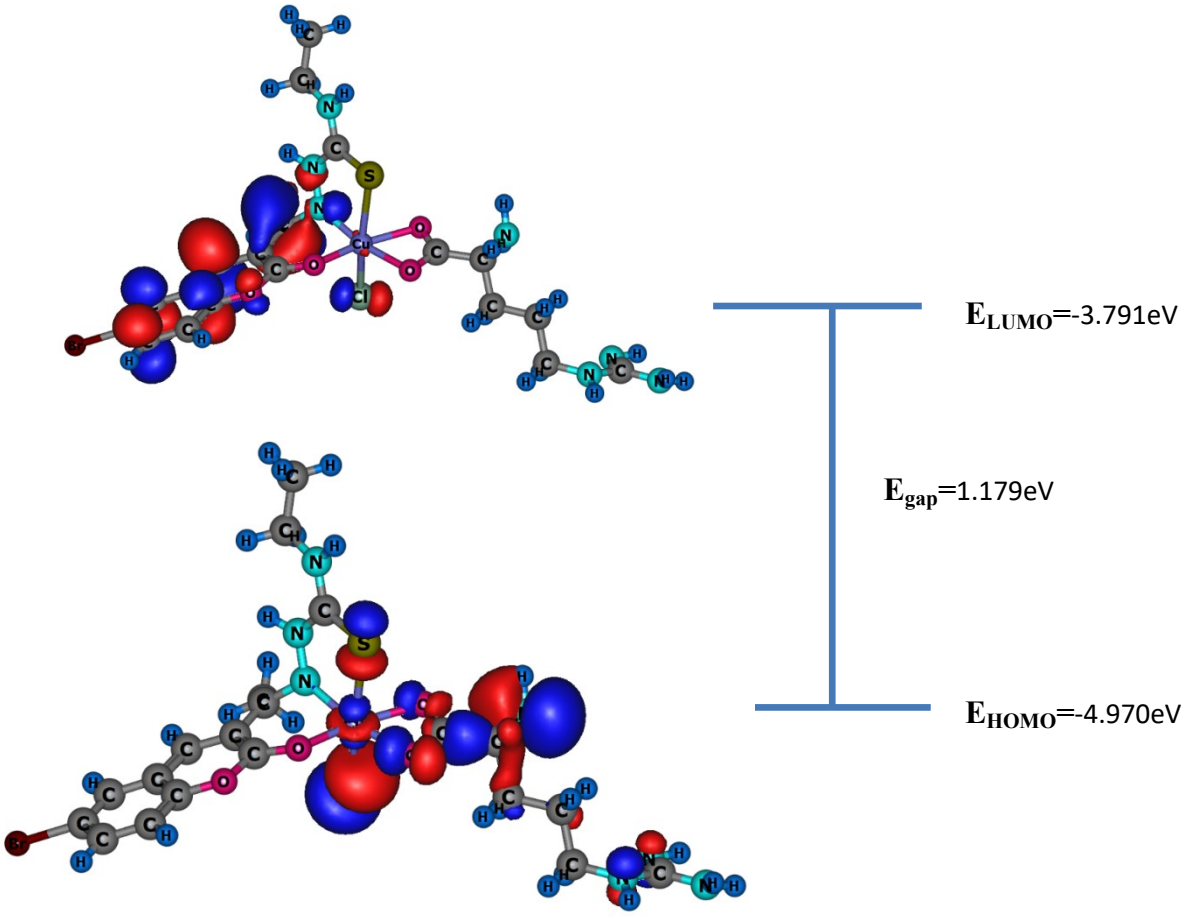

Fig. S33 HOMO-LUMO energy levels of RR1-Cu^{2+}-L-Arginine complex were calculated from Hartree level of theory (B).

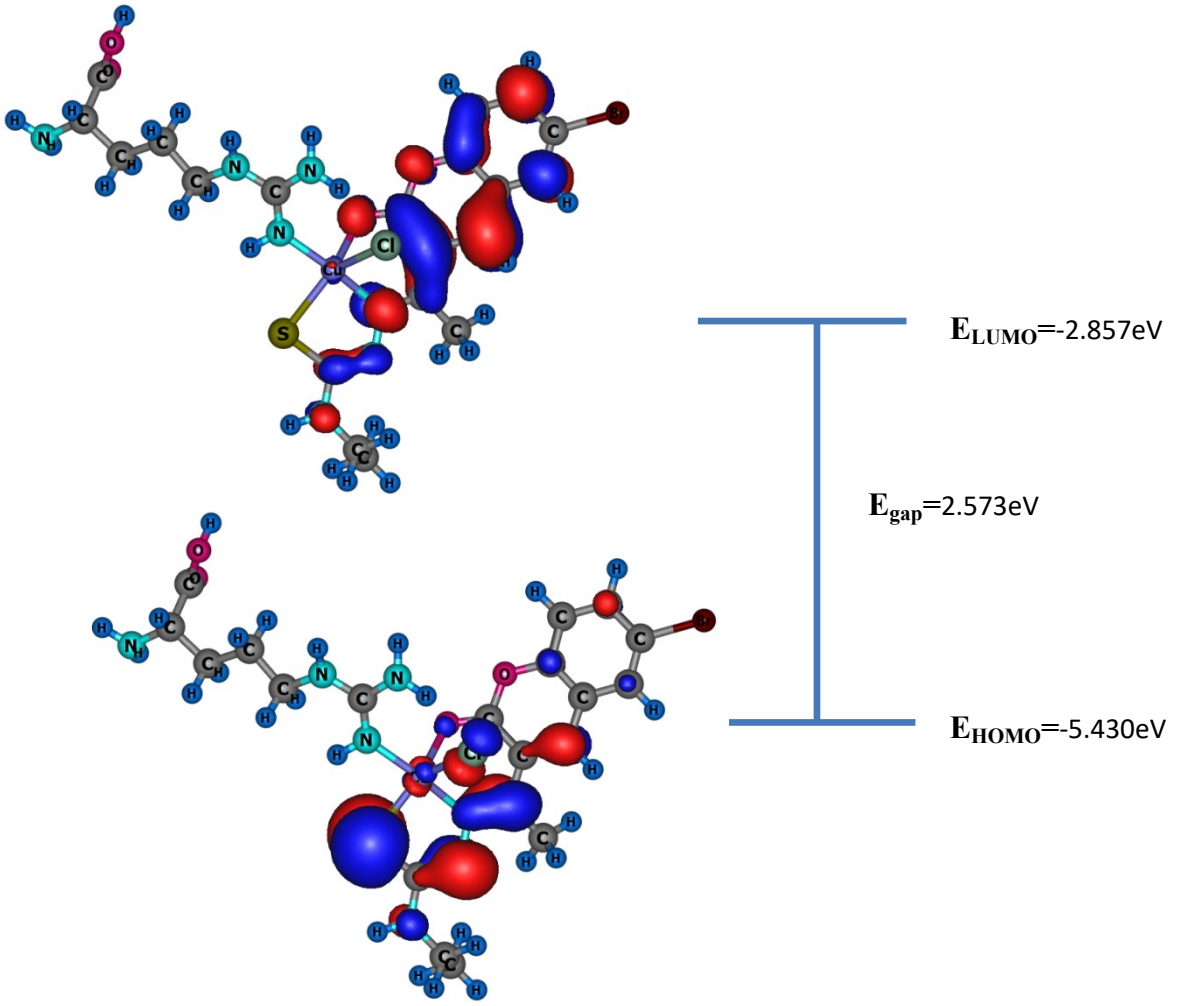

Fig. S34 HOMO-LUMO energy levels of RR1-Cu^{2+}-L-Arginine complex were calculated from Hartree level of theory (C).

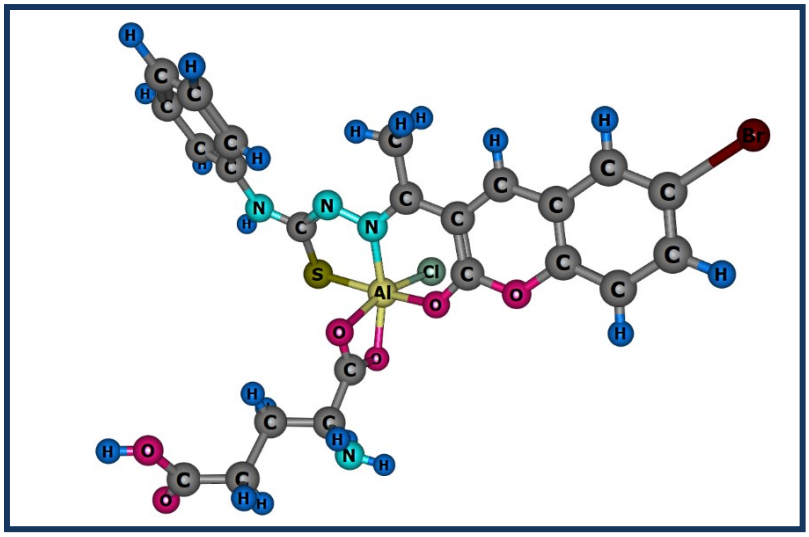

Fig.S35 Optimized structure of the RR2-Al^{3+}-L-Glutamic acid (E).

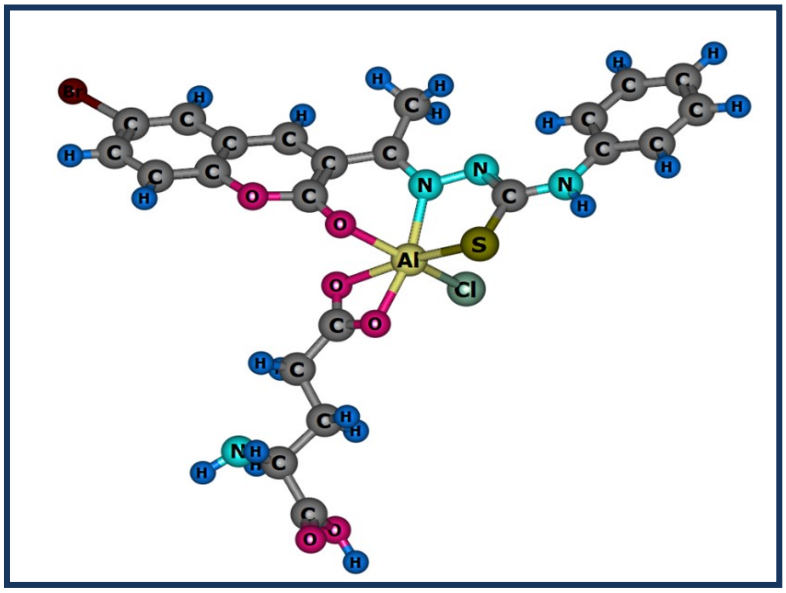

Fig.S36 Optimized structure of the RR2-Al^{3+}-L-Glutamic acid (F).

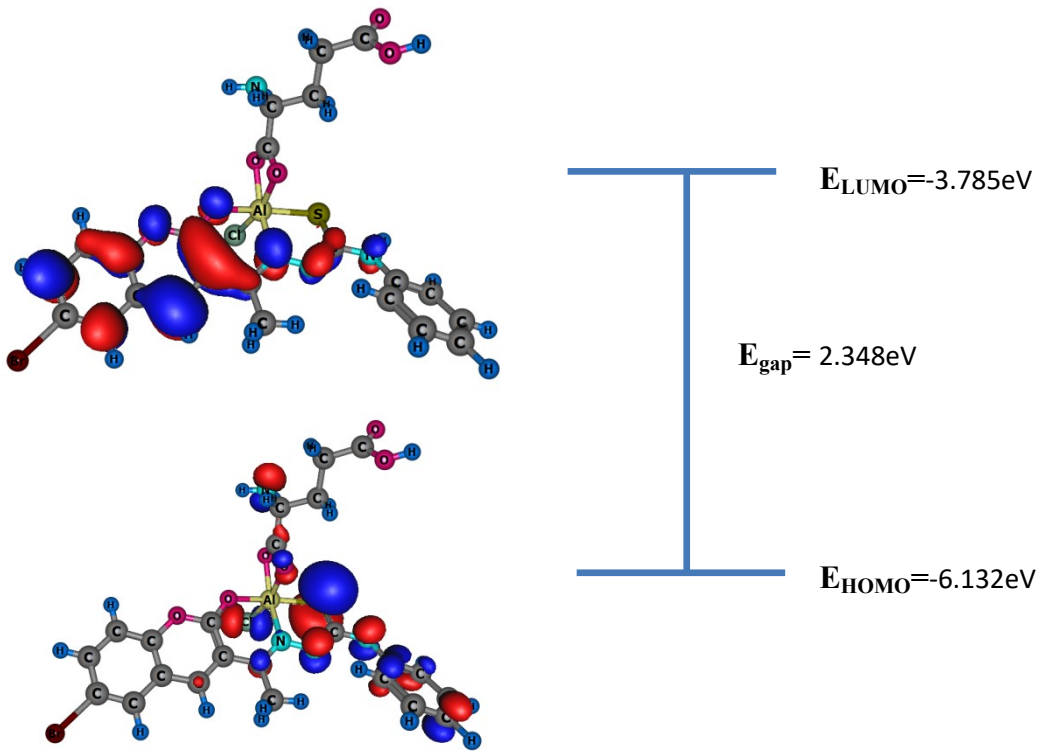

Fig.S37 HOMO-LUMO energy levels of RR2-Al^{3+}- L-Glutamic acid complex were calculated from Hartree level of theory (E).

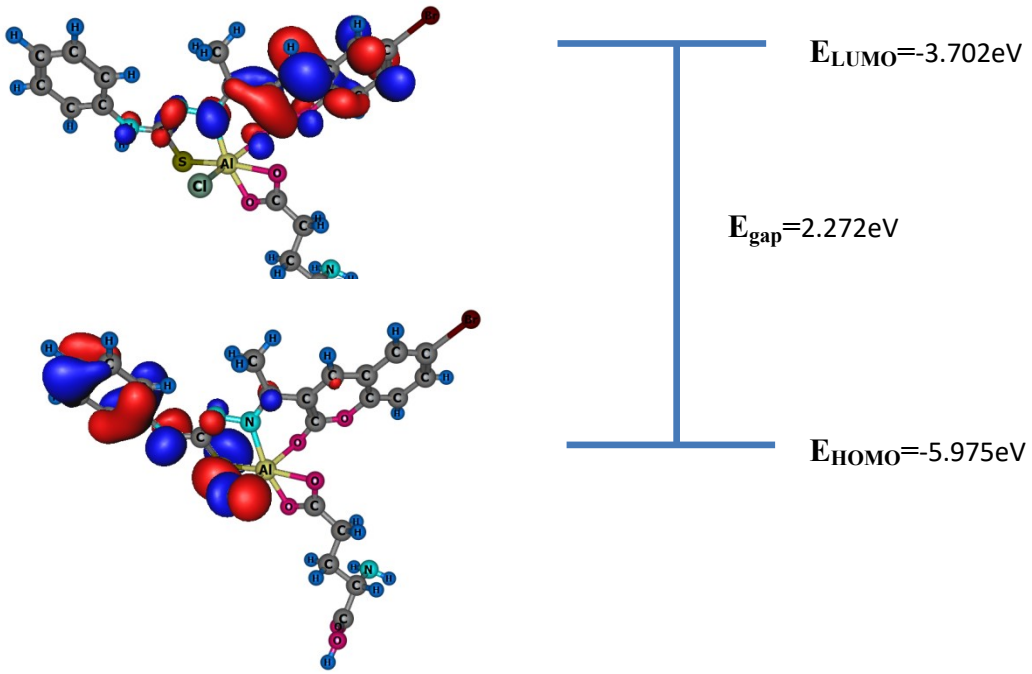

Fig. S38HOMO-LUMO energy levels of RR2-Al^{3+}-L-Glutamic acid complex were calculated from Hartree level of theory (F).

Table S2. Minimum energy (in Hartree) of the stable structures.

Compound	Energy (Hartree)	Relative energy (kcal/mol)
RR2-Al^{3+}	-1063.628	0
RR2-Al^{3+}-L-Glutamic acid	-1599.657	
RR2-Al^{3+}-L-Glutamic acid (1)	-1599.627	18.83
RR2-Al^{3+}-L-Glutamic acid (2)	-1599.616	27.73
RR1-Cu^{2+}	-1105.875	0
RR1-Cu^{2+}-L-Arginine	-1696.740	
RR1-Cu^{2+}-L-Arginine (1)	-1696.646	58.99
RR1-Cu^{2+}-L-Arginine (2)	-1696.634	66.52

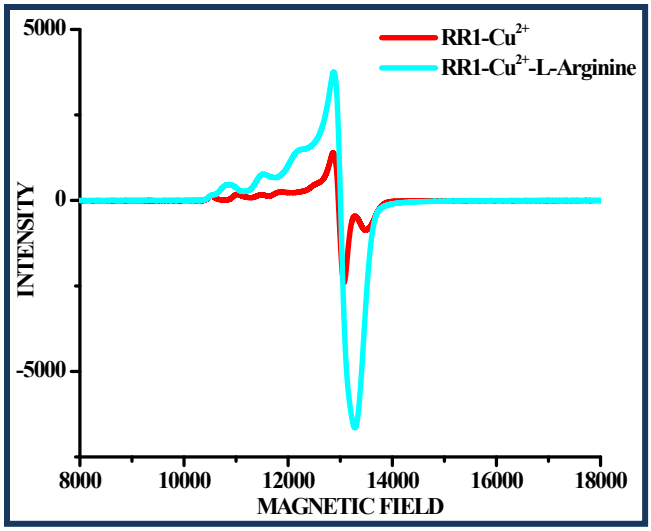

Fig. S39EPR spectra of **RR1-Cu^{2+}** and **RR1-Cu^{2+}-L-arginine (at 77K)**.

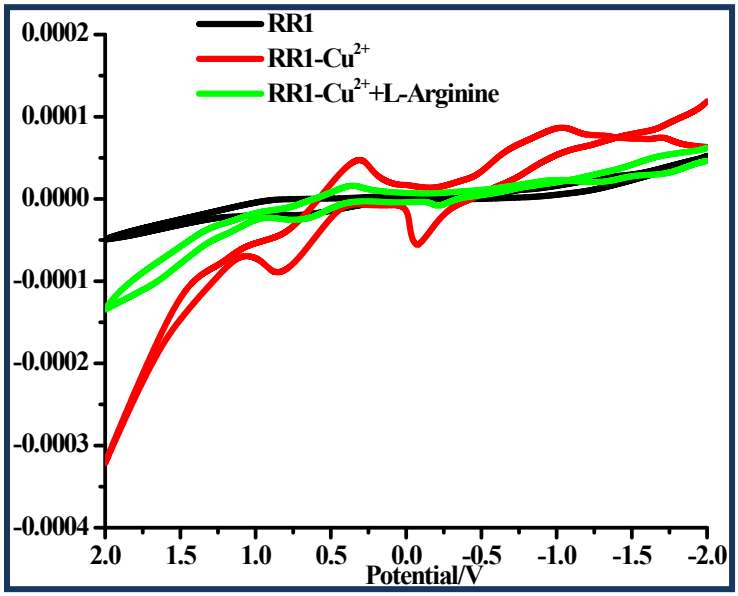

Fig. S40 Cyclic Voltammogramsof **RR1**, **RR1-Cu^{2+}**and**RR1-Cu^{2+}-L-arginine**.

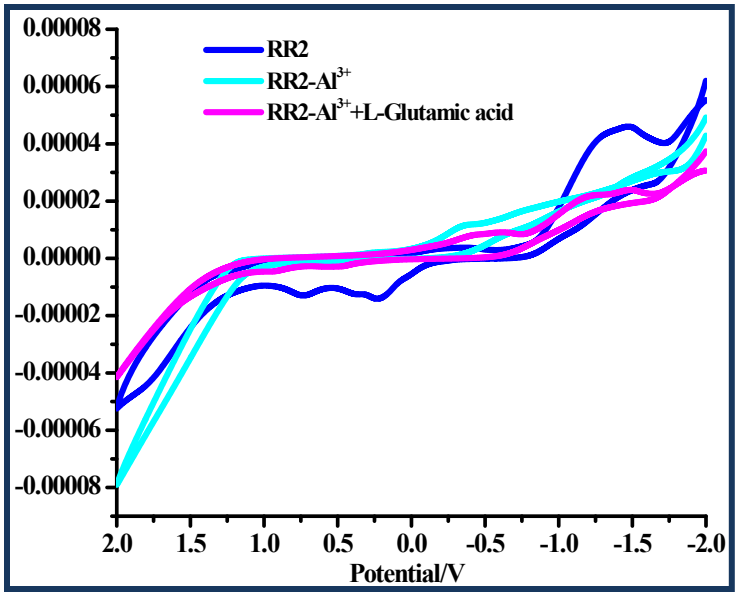

Fig.S41 Cyclic Voltammogramsof **RR2**,**RR2-Al^{3+}** and**RR2-Al^{3+}-L-glutamic acid**.

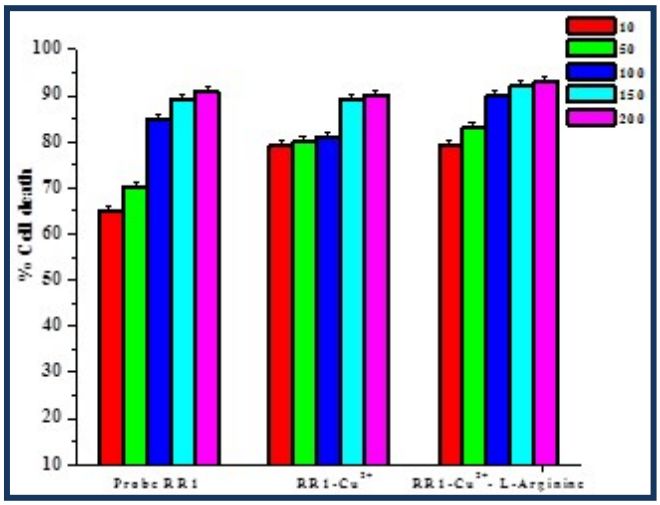

Fig. S42MDA-MB-231 cells were treated with different concentrations of probe **RR1**; **RR1-Cu^{2+}** and **RR1-Cu^{2+}- L-arginine**.

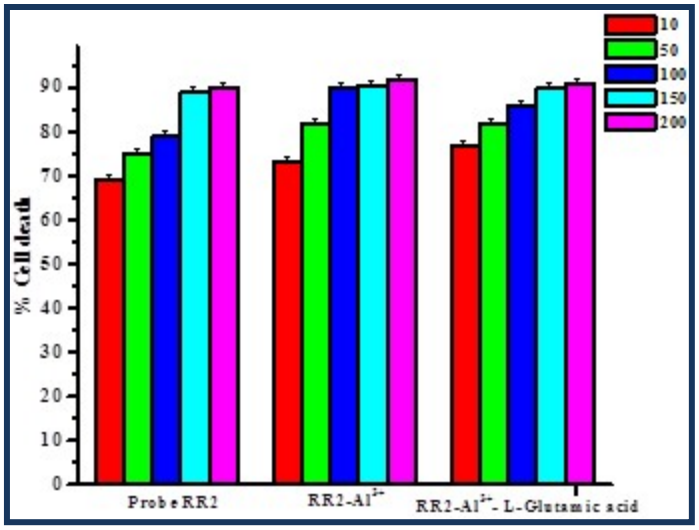

Fig. S43MDA-MB-231 cells were treated with different concentrations of probe **RR2**; **RR2-Al^{3+}** and **RR2-Al^{3+}-L-glutamic acid**.

References

1. A. I. Vogel, *Textbook of Practical Organic Chemistry, 5th ed*., Longman, London, 1989, **268**
2. SAINT V8.34A Bruker AXS Inc, Madison, WI, 2013.
3. G. M. Sheldrick, *Acta Cryst*., 2015, **A71**, 3.
4. G. M. Sheldrick, *ActaCryst*.,2015, **C91**, 9.
5. A. L. Spek, *ActaCryst*.,2009, **D65**, 148-155.
6. L. J. Farrugia, *J. Appl. Cryst*., 1999, **32,** 837.
7. O. V. Dolomanov, L. J. Bourhis, R. J. Gildea, J. A. K. Howard and H. Puschmann, *J. Appl. Cryst*., 2009, **42**, 339-341.
8. S. Brenner *Genetics,* 1974, **77**, 71.
9. T. Stiernagle, *Maintenance of C. elegans, WormBook.* 2006.
10. C. Elamathi, R.J. Butcher, A. Mohankumar, P. Sundararaj, A. Madankumar, P. Kalaivani, R. Prabhakaran, *Inorg. Chem. Front.,* 2019,**6**, 3237.
11. A. Kalaiarasi, C. Anusha, R. Sankar, S. Rajasekaran, J. John Marshal, K. Muthusamy, V. Ravikumar, *J. Agric. Food Chem*., 2016,**64**, 9542-9550.

12. A. Chidambaram, A. Sekar, R.K. Chidambaram, K. Arunachalam, R. Vilwanathan, *Investigational New Drugs*, 2017,**35(6)**, 691-705.